Microbiology (2016), **162**, 909–920 DOI 10.1099/mic.0.000278

Editor's Choice

ClpXP and ClpAP control the *Escherichia coli* division protein ZapC by proteolysis

Monika S. Buczek,[1,2] Andrea L. Cardenas Arevalo[1] and Anuradha Janakiraman[1,2]

Correspondence
Anuradha Janakiraman
anuj@ccny.cuny.edu

[1]Department of Biology, MR 526, The City College of CUNY, New York, NY 10031, USA
[2]The Graduate Center of CUNY, New York, NY 10016, USA

Received 9 November 2015
Accepted 13 March 2016

The bacterial FtsZ-ring is an essential cytokinetic structure under tight spatiotemporal regulation. In *Escherichia coli*, FtsZ polymerization and assembly into the Z-ring is controlled on multiple levels through interactions with positive and negative regulators. Among these regulatory factors are ZapC, a Z-ring stabilizer, and the conserved protease ClpXP, which has been shown to degrade FtsZ protofilaments in preference to FtsZ monomers. Here we report that ZapC and ClpX interact in a protein–protein interaction assay, and that ZapC is degraded in a ClpXP-dependent manner *in vivo*. The SspB adaptor protein is not required for targeting ZapC to the ClpXP proteolytic machinery. A mutation disrupting the *zapC ssrA*-like sequence (*zapC*^{DD}) stabilizes ZapC consistent with a reduction in ClpXP-mediated ZapC degradation. ZapC^{DD} retains the ability to interact with FtsZ and to promote bundling *in vitro* indicating that WT ZapC contains discrete FtsZ and ClpX recognition motifs. Additionally, ClpAP complexes are sufficient for degradation of ZapC in the absence of ClpX *in vivo*. Further, chromosomal expression of *zapC*^{DD} suppresses filamentation of the temperature-sensitive *ftsZ84* mutant, confirming the role of ZapC as a Z-ring stabilizer. Lastly, changes in ClpXP and ZapC levels lead to cell division effects, likely through their roles in modulating FtsZ assembly dynamics. Taken together, our results indicate that the Z-ring stabilizer ZapC is a substrate of both ClpXP and ClpAP *in vivo*. Our data also point to a more complex regulatory circuit that integrates FtsZ, ClpXP and ZapC in achieving Z-ring stability in *E. coli* and related species.

INTRODUCTION

In most bacteria, cell division is initiated by polymerization of FtsZ into a membrane-associated cytokinetic ring (Z-ring) at the midcell division site (Bi & Lutkenhaus, 1991). The Z-ring scaffold then recruits numerous proteins into a multiprotein complex known as the divisome (de Boer, 2010; Lutkenhaus *et al.*, 2012). FtsZ is a self-activating GTPase that assembles into single-stranded polymers (protofilaments) when bound to GTP (Erickson *et al.*, 2010). Hydrolysis of the bound nucleotide leads to depolymerization of the FtsZ protofilaments (Erickson *et al.*, 2010; Mukherjee & Lutkenhaus, 1998). As FtsZ levels are essentially constant throughout the cell cycle, spatiotemporal control of division is exercised largely through the assembly/disassembly of the Z-ring (Rueda *et al.*, 2003; Weart & Levin, 2003). A number of proteins that interact with FtsZ contribute to its function by modulating the dynamics of FtsZ-assembly (Adams & Errington, 2009; Huang *et al.*, 2013; Lutkenhaus *et al.*, 2012; Ortiz *et al.*, 2016). However, the precise molecular nature of the protein–protein interactions between FtsZ and FtsZ-regulators that yield a stable but dynamic Z-ring is not completely understood as yet.

A common mechanism of the regulation of many fundamental cellular processes, including cytokinesis, is proteolysis of key substrates. In *Escherichia coli*, FtsZ is degraded by the widely conserved ATP-dependent protease, ClpXP (Camberg *et al.*, 2009). Polymeric FtsZ is thought to be the primary substrate, suggesting that ClpXP may influence Z-ring dynamics by altering the balance of FtsZ monomer/polymer pools in the cell (Camberg *et al.*, 2009). ClpXP is composed of two subunits: ClpX, an AAA+ family ATPase, and ClpP, a 14-subunit serine peptidase (Baker & Sauer, 2012; Wickner *et al.*, 1999). ClpX selectively recognizes multiple cellular substrates including those associated with cell division and translocates these proteins into the

Abbreviations: Amp, ampicillin; BACTH, bacterial two-hybrid; Kan, kanamycin.

Four supplementary figures and two supplementary tables are available with the online Supplementary Material.

degradation chamber of the ClpP peptidase (Baker & Sauer, 2012; Gottesman *et al.*, 1995). *In vitro*, ClpXP can degrade FtsZ dependent upon either one of two regions of FtsZ: one in the FtsZ unstructured linker region, and the second in the FtsZ conserved carboxy-terminal peptide (CCTP) domain. This second site partially overlaps the recognition sites of FtsZ-regulatory proteins MinC (topological specificity inhibitor), ZipA (essential membrane tether and stabilizer), FtsA (essential membrane tether and stabilizer) and ZapD (FtsZ-ring stabilizer) (Camberg *et al.*, 2014; Durand-Heredia *et al.*, 2012; Haney *et al.*, 2001; Shen & Lutkenhaus, 2009). Both ZipA and FtsA anchor FtsZ to the membrane via interaction with the FtsZ CCTP in *E. coli*, but only ZipA interferes with ClpXP-mediated FtsZ degradation (Pazos *et al.*, 2013). *In vivo*, FtsZ degradation is reduced in the absence of MinC, suggesting that MinC may also influence ClpXP-mediated FtsZ inhibition (Camberg *et al.*, 2011). In addition to its role in the ClpXP complex, ClpX alone acts as an ATP-dependent chaperone to remodel protein substrates (Baker & Sauer, 2012). Control of FtsZ assembly mediated by ClpXP or ClpX alone has been observed in model bacteria including *Bacillus*, *Caulobacter*, *Staphylococcus* and *Mycobacterium* (Dziedzic *et al.*, 2010; Feng *et al.*, 2013; Haeusser *et al.*, 2009; Weart *et al.*, 2005; Williams *et al.*, 2014). Notably, the precise mechanisms by which ClpX, alone or together with ClpP, influences FtsZ assembly in these bacteria are varied and are likely dependent on their specific environmental niches.

In addition to FtsZ, a number of Z-ring regulators were identified as putative ClpXP substrates in two independent proteomic studies where endogenous *E. coli* substrates were trapped in the proteolytic chambers of inactive ClpP proteases ($ClpP^{trap}$) and subsequently identified via mass spectrometry (Flynn *et al.*, 2003; Neher *et al.*, 2006). Among those proteins predicted to be ClpXP targets are ZapC, FtsA, MinD (division site-selection factor) and SulA (DNA damage induced FtsZ inhibitor) (Dajkovic *et al.*, 2008; Durand-Heredia *et al.*, 2011; Hale *et al.*, 2011; Lutkenhaus & Donachie, 1979; Park *et al.*, 2011; Pichoff & Lutkenhaus, 2005; Raskin & de Boer, 1999).

ZapC is a ~20 kD gammaproteobacterial cytoplasmic protein that stabilizes FtsZ polymers (Durand-Heredia *et al.*, 2011; Hale *et al.*, 2011). ZapC interacts directly with FtsZ, promotes FtsZ bundling and suppresses the GTPase activity of FtsZ *in vitro* (Durand-Heredia *et al.*, 2011; Hale *et al.*, 2011). The recent structure of ZapC reveals a two-domain protein with amino acid residues in both domains implicated in binding FtsZ (Ortiz *et al.*, 2015; Schumacher, *et al.*, 2016). In *E. coli*, a *zapC* mutant displays mild division defects compared to WT, but when combined with deletion of one or more of the Z-ring-associated positive regulators, *zapA*, *zapB* or *zapD*, or removal of the inhibitor MinC, *zapC* mutants exhibit cellular division defects and aberrant Z-ring morphologies indicating that ZapC promotes FtsZ-ring stability redundantly with other factors (Durand-Heredia *et al.*, 2011; Hale *et al.*, 2011). Prior work has shown that overexpression of ZapC leads to hyperstable Z-ring assemblies and filamentation without affecting steady-state FtsZ levels (Durand-Heredia *et al.*, 2011; Hale *et al.*, 2011). Little is known about the regulation of ZapC itself, but the intracellular levels are considered to be low and it is predicted to be a substrate of ClpXP in *E. coli* (Flynn *et al.*, 2003; Li *et al.*, 2014). Consistent with this latter observation, the ZapC sequence encodes both an N-terminal ClpX recognition sequence (^{1}MRIK-X_6-W^{11}) and a C-terminal *ssrA*-like sequence (^{178}QAV^{180}) (Flynn *et al.*, 2003). The well-characterized *ssrA* tag, which bears the sequence AANDENYALAA, is added co-translationally to the C-terminus of a nascent polypeptide by the tmRNA ribosome rescue system when ribosomes stall during translation (Karzai *et al.*, 2000; Keiler *et al.*, 1996).

Together, these studies suggest that proteolysis is an important general mechanism for restructuring the divisome and influencing FtsZ assembly dynamics through the degradation of not only FtsZ but also its regulators. Using *in vivo* proteolysis assays of WT and mutant ZapC proteins, we show that ZapC is a bona fide ClpP substrate in *E. coli*. A protease-resistant *zapC* mutant, $zapC^{DD}$, suppresses filamentation in a thermosenstive *ftsZ* mutant underscoring a positive role for ZapC in FtsZ assembly. Additionally, $zapC^{DD}$ protects against ClpXP overexpression-related filamentation, offering further support that ClpP-mediated proteolytic control of ZapC contributes to Z-ring assembly dynamics.

METHODS

Media and strains. Bacteria were grown in LB (0.5 % NaCl) broth or agar plates with the antibiotics indicated at 37 °C unless otherwise mentioned. Antibiotics were used at the following concentration unless otherwise noted: ampicillin (Amp), 100 μg ml^{-1}; kanamycin (Kan), 50 μg ml^{-1}; spectinomycin, 100 μg ml^{-1} and chloramphenicol, 25 μg ml^{-1}. All strains and plasmids used in this study are listed in Tables 1 and S1 (available in the online Supplementary Material). All strains used are derivatives of MG1655. Primers used in the study are listed in Table S2.

Plasmid construction. Plasmid pBAD33 expressing *zapC* under the control of an arabinose-inducible promoter was constructed by amplifying *zapC* using the P5 YcbW-U forward and SUMO3 ZapC *Hin*dIII reverse primers. The PCR product was digested by PstI/*Hin*dIII endonucleases and ligated into pBAD33 vector treated with the same restriction enzymes. The resulting clones were verified by Sanger sequencing (Genewiz). Plasmid pBAD33-$zapC^{DD}$ was created from pBAD33-*zapC* by Quickchange mutagenesis (Agilent) using the *zapC* A179D V180D forward and reverse primers. To avoid potentially confounding effects of mutations in the vector backbone introduced during mutagenesis, after sequencing verification, the mutagenized region of the plasmid was excised using KpnI and HindIII and the resulting fragment re-ligated into the same sites of the pBAD33 parent vector. Plasmid pNG162-*zapC* was constructed by amplifying *zapC* with pNG162 ZapC BamHI forward and pNG162 ZapC *Hin*dIII reverse primers. The PCR product was digested with BamHI and HindIII and ligated into the same sites of the pNG162 vector.

Fusion plasmids for bacterial two-hybrid (BACTH) assays were constructed as follows: PCR amplification of *zapC* and $zapC^{DD}$ was conducted using primers T25-ZapC 5P and T25 ZapC 3P or T25-$ZapC^{DD}$ 3P. Amplified DNA was digested with BamHI and EcoRI restriction endonucleases and ligated into the same sites in the pKT25 vector.

Table 1. Strains and plasmids used in the study

Strain or plasmid	Relevant genotype*	Source or reference†
BTH101	*cya99 araD139 galE15 galK16 rpsL1* (Str^R) *hsdR2 mcrA1 mcrB1*	Karimova *et al.* (2000)
BW25141	*lacI*^{q}*rrnB*$_{T14}$ Δ*lacZ*$_{WJ16}$ Δ*phoBR580 hsdR514* Δ*araBAD*$_{AH33}$ Δ*rhaBAD*$_{LD78}$ *galU95 end-A*$_{BT333}$ *uidA*(Δ*MluI)* :: *pir*$^+$*recA1*	Datsenko & Wanner (2000)
BW25311	*lacI*^{q}*rrnB*$_{T14}$ Δ*lacZ*$_{WJ16}$ *hsdR514* Δ*araBAD*$_{AH33}$ Δ*rhaBAD*$_{LD78}$	Datsenko & Wanner (2000)
MG1655	F$^-$λ$^-$*rph1 ilvG rfb-50*	Lab stock
MGZ84	MG1655 *ftsZ84* (Ts) *leu* :: Tn10	Manjula Reddy (CCMB)
TB28	MG1655 Δ*lacIZYA* :: *frt*	Bernhardt & de Boer (2004)
XL10-Gold	*endA1 glv44 recA1 thi1 gyrA96 relA1 lac* Hte Δ(*mcr*A)*183* Δ(*mcrCB-hsdSMR-mrr)173* F′ [*proAB lacI*^{q} *Z*Δ*M15* Tn*10* (Tet^R) *amy* Cm^R]	Agilent
AC01-18	JD505 Δ*clpX* :: Kan^R	
AC01-20	JD505 pClpXP	
AC01-22	JD505 pBR322	
AJ-S08	MG1655 Δ*clpA* :: Kan^R	
HVF1	MG1655 Δ*sspB* :: Kan^R	
HVF2	HVF1 pBAD33-*zapC*	
JD407	MG1655 Δ*clpX* :: Kan^R	
JD409	MG1655 Δ*clpP* :: Kan^R	
JD436	MG1655 pBAD33-*zapC*	
JD454	MG1655 pBAD33-*zapC L22P*	
JD455	MG1655 pBR322	
JD456	MG1655 pClpXP	
JD458	JD436 pBR322	
JD459	JD436 pClpXP	
JD474	MG1655 pBAD33-*zapC*^{DD}	
JD476	JD474 pBR322	
JD479	JD474 pClpXP	
JD505	TB28 Δ*zapC* :: *frt*	
LT57	TB28 pNG162-*zapC*	
MB04	JD409 pBAD33-*zapC*	
MB06	JD407 pBAD33-*zapC*	
MB10	JD407 pBAD33-*zapC*^{DD}	
MB13	JD409 pBAD33-*zapC*^{DD}	
MB94	AJ-S08 pBAD33-*zapC*	
MB99	JD505 Δ*clpP* :: Kan^R	
MB103	JD505 Δ*clpA* :: Kan^R	
MB110	MB99 pNG162-*zapC*	
MB115	MG1655 Δ*clpA* :: <*frt*>	
MB143	MB115 Δ*clpX* :: Kan^R	
MB146	MB143 pBAD33-*zapC*	
MB181	MG1655 *zapC*^{DD}-Kan^R	
MB184	MGZ84 Δ*clpP* :: Kan^R	
MB188	MGZ84 Δ*clpX* :: Kan^R	
MB199	MGZ84 *zapC*^{DD}-Kan^R	
MB203	MB181 pClpXP	
Plasmid		
AC01-09	pKT25-ZapC; Kan^R	
AC01-10	pKT25-ZapC^{DD}; Kan^R	
AC01-58	pUT18C-ClpX; Amp^R	
pBAD33	pACYC184 ori; P_{BAD}; Cm^R	Lab stock
pBR322	pMB1 ori; Amp^R Tet^R	Lab stock
pClpXP	pBR322 *clpX clpP*; native promoter; Amp^R	Michael Maurizi (NIH)
pCP20	pSC101 ori; *c*I875 *repA*(Ts) P_R:: *flp*; Amp^R Cm^R	Datsenko & Wanner (2000)

Table 1. cont.

Strain or plasmid	Relevant genotype*	Source or reference†
pDONR221	ColE1 ori; Kan^R; Gateway Donor vector	Thermo Fisher
pKD4	R6K ori; *bla frt<kan>frt*	Datsenko & Wanner (2000)
pKD46	pSC101 ori*Ts*; *araC-*P_{araB} *gam bet exo*; Amp^R	Datsenko & Wanner (2000)
pKT25	pACYC184/15A ori; P_{lac} :: *T25*-MCS; Kan^R	Tom Bernhardt (HMS)
pNG162	pSC101 ori; $lacI_Q$ P_{204}; Spc^R	Goehring *et al.* (2006)
pUT18C-DEST	pBR322 ori; P_{lac}:: *T18*-MCS; Amp^R	Scot Ouellette (USD)

*The Kan^R cassette is flanked by *frt* sites for removal by FLP recombinase. A *frt* scar remains following removal of the cassette using FLP expressed from pCP20.
†This work unless otherwise mentioned.

Resulting clones were verified by sequencing (Genewiz) and transformed into XL10 Gold (Agilent) (contains *lacI* repressor) to prevent leaky expression from the pKT25 plasmid. To obtain a T18–*clpX* fusion, *clpX* was amplified using *clpX* 5P-GW and *clpX* 3P-GW primers and recombined into the pUT18C-DEST vector via Gateway (Thermo Fisher Scientific).

Bacterial two-hybrid (BACTH) assays. Appropriate pairs of T25 and T18 fusion plasmids were co-transformed into BTH101 and plated on LB Amp Kan plates for 48 h at 30 °C. The β-galactosidase activities of the strains were measured essentially as described previously (Karimova *et al.*, 1998, 2000). Briefly, overnight cultures grown in LB with appropriate antibiotics in the presence of 0.5 mM IPTG at 30 °C were pelleted, washed in PM2 buffer and diluted 1 : 5 in the same buffer and OD_{600} values noted (Karimova, *et al.*, 2000). Cell cultures were permeabilized by adding 35 µl chloroform and a drop of 0.1 % SDS per 2.5 ml of the diluted cell suspensions, vortexed for 10 s and shaken at 37 °C for 40 min. To obtain enzymatic activities, 0.1 ml of the permeabilized cells was added to 0.9 ml PM2 buffer and the reactions were initiated by adding 0.25 ml 0.4 % ONPG pre-equilibrated at 30 °C (Karimova *et al.*, 2000). After sufficient yellow colour had developed, each reaction was stopped by adding 0.5 ml 1 M Na_2CO_3 and the time noted. At this point, OD_{420} and OD_{550} values were also recorded for each culture. Enzymatic activity is reported in Miller units and calculated as described by Miller (1972).

Antibiotic chase experiments. An *in vivo* protein turnover assay using antibiotic chase was performed to examine the stability of WT ZapC or mutant $ZapC^{DD}$ over a period of ~2 h in WT or *clpX*, *clpA*, *clpP* or *clpX clpA* mutant cells. ZapC stability was also monitored in cells overexpressing ClpXP. The ClpXP overexpression plasmid pClpXP contained the *clpX clpP* operon under the control of the native promoter in the pBR322 vector backbone and is thought to result in ~4-fold overexpression of ClpX and ~75-fold overexpression of ClpP (Camberg *et al.*, 2009). Overnight cultures of strains bearing ZapC or $ZapC^{DD}$ *in trans* grown in LB with appropriate antibiotics at 37 °C were back-diluted 1:100 into the same media and grown to OD_{600} of ~0.3 at which point 0.02 % L-arabinose was added to induce ZapC or $ZapC^{DD}$expression for 30 min. Chromosomally encoded WT *zapC* or $zapC^{DD}$ strains were grown to an OD_{600} of ~0.6. At this point protein synthesis was stopped by the addition of spectinomycin at 200 µg ml^{-1} or chloramphenicol at 100 µg ml^{-1} and cultures grown for an additional 2 h. Cells were harvested immediately upon addition of antibiotic and every 15 or 30 min thereafter for a total period of 120 min for whole cell protein preparations. Cells were sampled at equivalent ODs to ensure the same amount of protein was loaded per lane. Proteins were analyzed on 15 % SDS-PAGE and immunoblotted. Rabbit polyclonal primary antibodies raised against ZapC and FtsZ peptides (Genscript) were used at 1 : 1000 and 1 : 10 000 dilutions, respectively. A rabbit polyclonal EF-Tu primary antibody (a gift of Michael Maurizi) was used at 1 : 50 000 as a loading control. An IR-conjugated secondary antibody at 1 : 10 000 (LI-COR) was used for detection in an Odyssey CLx Infrared imaging system. Intensity measurements were calculated using ImageQuant (LI-COR) software. All decay times were obtained using non-linear least squares fit to exponential decay curves using a single variable parameter (the decay time). The half-life ± SD values are included in the main text.

Creation of a $zapC^{DD}$ mutant at its native locus on the chromosome. A strain bearing a $zapC^{DD}$ mutant at the native locus on the chromosome was created by lambda recombineering essentially as described by Peters *et al.* (2011). A kanamycin cassette was amplified using pKD4 plasmid as a template with a *zapC* 3′-end sequence primer, $zapC^{DD}$-stop-pKD4-PS1, and a primer downstream of *zapC*, $zapC^{DD}$-downstream-pKD4-PS2. The resulting PCR product was verified by sequencing and used for recombineering into BW25311/pKD46 strain as described by Datsenko & Wanner (2000). The $zapC^{DD}$ mutant linked to the kanamycin marker was transferred into the WT (MG1655) background by P1 transduction (Miller, 1972).

Spot viability assays. Overnight cultures of *ftsZ84* (Ts) alone or in combination with $zapC^{DD}$, *clpX* or *clpP* mutants grown in permissive conditions, LB at 30 °C, were briefly centrifuged and resuspended in LB or LBNS (LB no salt). Cell suspensions were normalized to OD_{600}=1.0, serially diluted to 10^{-4}, and 6 µl from each dilution was spotted on LB or LBNS plates. The plates were incubated at 37 °C for ~16 h, at which point they were imaged (Syngene Gel-Doc system).

Cell length measurements. Overnight cultures of WT, mutants, or cells overexpressing ZapC, $ZapC^{DD}$ or ClpXP plasmids were grown at 37 °C in LB medium with the appropriate antibiotics. Cells were subcultured 1 : 100 and grown under the same conditions, and samples were harvested at OD_{600}=~0.6–0.8. Cells were imaged using a Nikon TiE microscope on 1 % agarose pads on glass slides. ObjectJ (NIH) was used to measure cell length from images as described by Durand-Heredia *et al.* (2012). Overnight cultures of strains bearing a *ftsZ84* (Ts) mutation were grown at 30 °C in LB, subcultured 1 : 100 in LB or LBNS media at 30 °C or 37 °C the next day and grown till OD_{600}=~0.7–0.8, at which point cells were imaged and cell lengths measured as described above.

RESULTS

ZapC and ClpX interact in a BACTH system

The FtsZ-stabilizer ZapC is a putative substrate of the ClpXP protease in *E. coli* and harbours a potential *ssrA*-like ClpX recognition motif (Flynn *et al.*, 2003). Therefore, we

sought to investigate whether ZapC is a direct substrate of the ClpXP protease complex. We first examined the conservation of ZapC *ssrA*-like sequences and identified two strongly conserved residues (Fig. 1a). We mutagenized these C-terminal residues in order to test their importance in interactions with ClpX and proteolysis *in vivo*. Next, we tested whether WT ZapC and a mutant variant of ZapC in which the *ssrA*-like tag sequences are altered [*ZapC*^{DD} (A179D, V180D)] display interaction with ClpX in a BACTH system. Our results indicate a robust interaction between ClpX and WT ZapC, and only a slightly reduced interaction (~3-fold) between ClpX and ZapC^{DD} (Fig. 1b). While these results are consistent with the proteomic screen data and support the notion that ZapC is a target of ClpX recognition in *E. coli*, they do not exclude the possibility of other ClpX binding sites on ZapC.

ZapC is degraded by ClpXP and ClpAP in *E. coli*

To examine more directly whether ZapC is a ClpXP proteolytic substrate *in vivo*, we performed an antibiotic chase protein turnover assay to monitor the stability of ZapC in cells overexpressing ClpXP, and in cells lacking either ClpX or ClpP. As endogenous levels of ZapC are barely detectable by our anti-ZapC primary antibody in WT cells, we used an arabinose-inducible plasmid-borne ZapC or ZapC^{DD} multicopy expression construct to measure turnover in this study. ZapC was rapidly degraded in the presence of increased ClpXP with a half-life ($t_{1/2}$) of 29 ± 6 min when compared to cells expressing the pBR322 vector alone ($t_{1/2}$=112 ± 7 min; Fig. 2a). In contrast, ZapC^{DD} levels were essentially stable over the same length of time in cells overexpressing ClpXP (Fig. 2a). We next tested ZapC degradation in cells lacking *clpX* or *clpP* compared to WT cells. As expected, ZapC turnover rates in WT cells paralleled those of ZapC degradation with the pBR322 vector alone with a $t_{1/2}$=101 ± 23 min (Fig. 2b). Of note, the half-life measures were similar ($t_{1/2}$=108 ± 7 min) with more sampling timepoints, increasing the confidence of turnover estimates reported in this work (Fig. S1). ZapC clearance rates in cells lacking *clpX* were similar to those in WT cells ($t_{1/2}$=99 ± 42); however, in *clpP* cells, ZapC was essentially stable over 120 min (Fig. 2b). The ZapC^{DD} mutant protein was stable in WT, *clpX* or *clpP* backgrounds, suggesting that the *ssrA*-like tag may be the major recognition motif of ClpXP-mediated degradation of ZapC in cells (Fig. 2b). These results are consistent with ZapC being a substrate of the ClpP proteolytic machinery *in vivo*.

Since ZapC degradation rates were similar in WT and *clpX* cells, we speculated that another cellular unfoldase may be replacing ClpX activity in a *clpX* mutant. Analogous to ClpXP, ClpAP preferentially degrades proteins with *ssrA* motifs (Lies & Maurizi, 2008). This raises the possibility that ClpAP complexes are sufficient for ZapC degradation in the absence of ClpX *in vivo*. To test this prediction, we measured ZapC turnover in *clpA* mutant cells via antibiotic

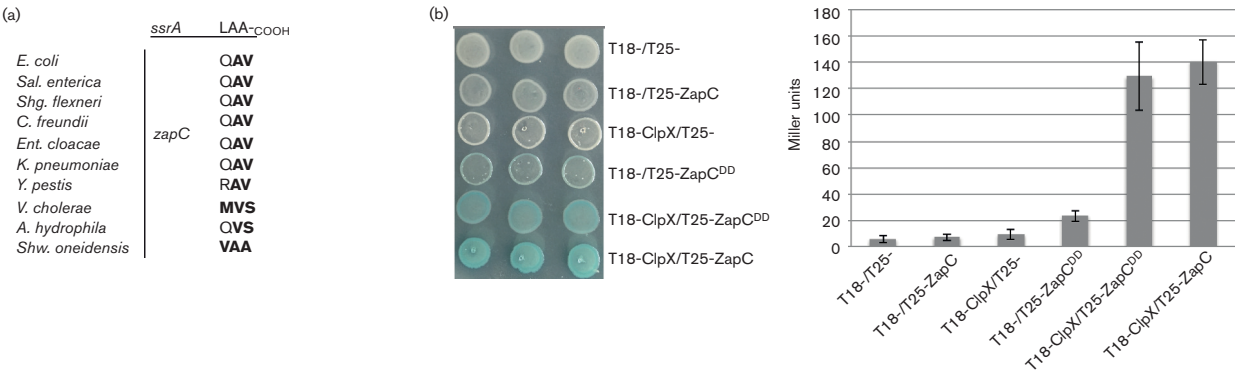

Fig. 1. ZapC and ClpX interact in a BACTH system. (a) Alignment of ZapC C-terminal *ssrA*-like sequences in select Enterobacterial, Aeromonad and Alteromonadale species shows conservation of residues in the terminal sequences. Similar sequences are in bold type. The sequences were obtained from the following bacteria: *E. coli* K-12 substrain MG1655 (NP_415466.4); *Salmonella enterica* subsp. *enterica* serovar *Typhimurium* LT2 (NP_460033.1); *Shigella flexneri* 2a (CEP58367.1); *Citrobacter freundii* (GAL42017.1); *Enterobacter cloacae* (CQR76953.1); *Klebsiella pneumoniae* (KHF69007.1); *Yersinia pestis* (Q7CHK5.1); *Vibrio cholerae* (KKP19598.1); *Aeromonas hydrophila* (A0KKK8.1); and *Shewanella oneidensis* (WP_011072541.1). (b) BACTH analysis of WT ZapC or a ZapC^{DD} variant fused to the C-terminal end of T25, and ClpX fused to the C-terminal end of T18 was conducted by transforming BTH101 cells with appropriate plasmid pairs encoding the fusion proteins. β-Galactosidase activities were monitored by colony phenotype on LB X-gal plates or in liquid cultures. For colony phenotypes, ~5 μl of overnight cultures of five or six transformants grown in LB Amp Kan were spotted on LB agar plates supplemented with Amp, Kan, X-Gal (40 μg ml^{-1}) and 0.5 mM IPTG and incubated at 30 °C for 24 h, at which point the plates were photographed. For β-galactosidase activity, cultures were grown and treated as described in Methods. Mean values and SD of at least three independent trials are reported in Miller units. T25- and T18- represent unfused vectors.

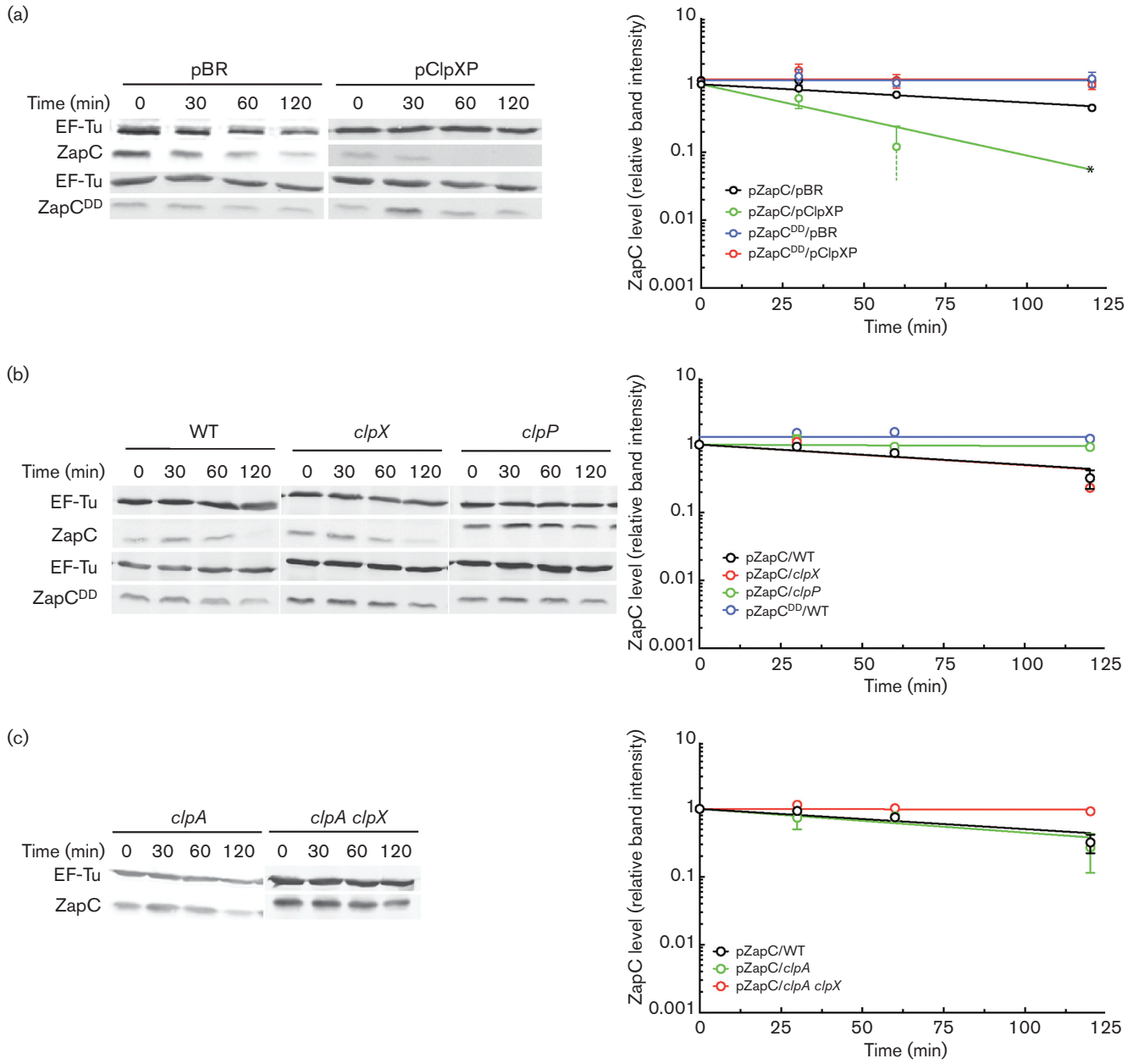

Fig. 2. ZapC is a substrate of ClpP-mediated proteolysis in the cell. (a) *In vivo* protein degradation assays were monitored by an antibiotic chase experiment as described in Methods. ZapC or ZapC^{DD} was expressed from an arabinose-inducible vector and ClpXP was constitutively expressed from its native promoter in a pBR322 vector as described in Methods. Cells expressing the pBR322 vector backbone alone (JD458) show ZapC degradation, which is amplified upon overexpression of ClpXP (JD459). A ZapC^{DD} variant bearing mutations in the C-terminal *ssrA*-like sequence (A179D V180D) is stable upon overexpression of ClpXP (JD479) compared to cells bearing the vector alone (JD476). A representative immunoblot with a graph of the relative band intensities as a function of time is shown. Band intensities are normalized to the loading control (EF-Tu) and reported relative to time-point zero. Quantification of triplicate assays is reported with mean values and SD of the decay times were obtained using non-linear least squares fits to exponential decay curves as described in the text. An asterisk (*) represents a non-detectable value set to zero for purpose of the fit. The dotted line at the 60 min time point represents a lower bound of the error that extends beyond zero. The data are plotted on a semi-log scale for visual representation only. (b) ZapC undergoes degradation in WT (JD436) and *clpX* (MB06) cells but is stabilized in a *clpP* mutant (MB04). A ZapC^{DD} variant is stable in all backgrounds (strains: JD474, MB10 and MB13). Only data points for ZapC^{DD} in the WT background are included in the graph for clarity. Quantification was done as reported above. (c) ZapC is a substrate of *clpA* (MB94) *in vivo* but is stable in a *clpX clpA* double mutant (MB146). Quantification was done as reported above. The WT curve from (b) is included for comparison.

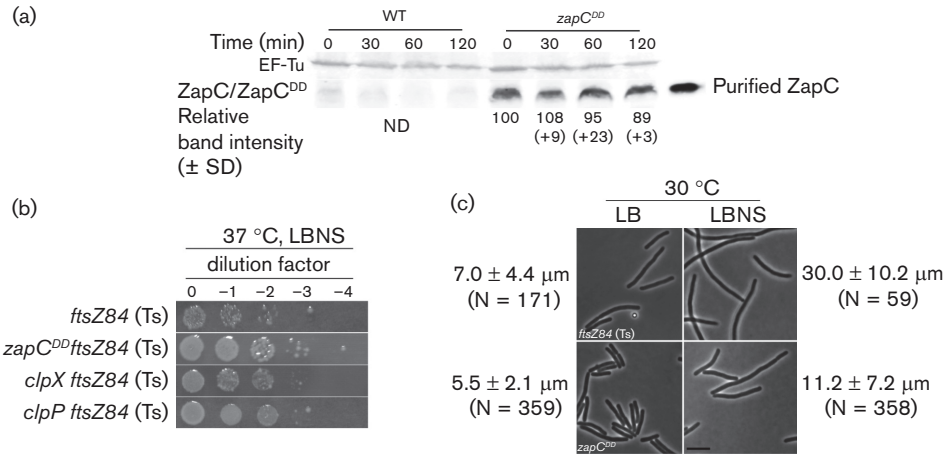

Fig. 3. Chromosomal expression of ZapC^{DD} is stable and suppresses *ftsZ84* (Ts) thermosensitive phenotypes *in vivo*. (a) ZapC^{DD} levels as expressed from the chromosome (MB181) are stable over a period of 120 min. WT ZapC is not detectable (ND) under the same conditions. An aliquot of purified tagless ZapC was run alongside to enable identification of ZapC^{DD} from whole cell lysates. Band intensities were normalized to loading control (EF-Tu) and reported relative to time-point zero. A representative blot with mean ZapC^{DD} band intensities ± SD of three independent trials is shown. (b) A *zapC^{DD}* mutant, or removal of *clpX* or *clpP*, partially suppresses *ftsZ84* (Ts) thermosensitivity. Overnight cultures of *ftsZ84* (Ts) (MGZ84), *zapC^{DD} ftsZ84* (Ts) (MB199), *clpX ftsZ84* (Ts) (MB188) and *clpP ftsZ84* (Ts) (MB184) grown under permissive conditions in LB at 30 °C were normalized to OD_{600}=1.0, serially diluted, and 6 μl aliquots of log dilutions were spot-plated on LBNS. Plates were incubated for ~16 h at 37 °C and imaged. (c) Overnight cultures of *ftsZ84* (Ts) (MGZ84) (top panels) and *zapC^{DD} ftsZ84* (Ts) (MB199; bottom panels) grown under permissive conditions in LB at 30 °C were subcultured into LB or LBNS media at 30 °C and grown till OD_{600}=0.7–0.8, at which point cells were imaged. Expression of *zapC^{DD}* suppresses filamentation of the *ftsZ84* (Ts) mutant under both growth conditions. Mean cell lengths ± SD are reported and were measured as described in Methods. N, total number of cells measured. Bar, 5 μm.

chase assays. Similar to turnover in *clpX* cells, ZapC stability in *clpA* cells was unaltered compared to WT ($t_{1/2}$=86 ± 20 min; Fig. 2c). Based on the ZapC stability observed in ClpP cells, we hypothesized that ZapC should be essentially stable in a *clpX clpA* double mutant. Indeed, we observed that ZapC levels are constant over the 120 min assay period (Fig. 2c). The *in vivo* protein stability assays indicate that ZapC is a proteolytic substrate of both ClpX and ClpA dependent on ClpP.

ClpXP-mediated ZapC degradation is SspB independent

The adaptor protein SspB contributes to ClpXP-mediated degradation of *ssrA*-tagged proteins by enhancing target recognition by ClpX (Levchenko *et al.*, 2000). The SspB adaptor recognizes residues in the *ssrA* tag that overlap with those of ClpA but not of ClpX recognition, perhaps leading to differential proteolytic activity *in vivo*. We therefore tested the contribution of SspB in the recognition of ZapC. Close examination of the ZapC C-terminal end sequence revealed no obvious SspB recognition residues, suggesting that SspB may have a limited role in ClpP-mediated ZapC degradation. Indeed, ZapC turnover rates in an *sspB* mutant were similar to those in the WT ($t_{1/2}$=98 ± 24 min), suggesting that SspB is not a major contributor in targeting ZapC to the ClpP proteolytic machinery.

Removal of both ZapC and ClpP contributes to increased heterogeneity in cell lengths

Imbalances in the levels of Z-ring regulatory proteins lead to division defects and altered cell lengths (Huang *et al.*, 2013; Ortiz *et al.*, 2016). ZapC stabilizes FtsZ polymers but ClpXP degrades FtsZ and, as we show here, both ClpXP and ClpAP degrade ZapC. Therefore, it is likely that there are synergistic division defects in strains with mutations in *zapC clpX*, *zapC clpA or zapC clpP* compared to WT and single mutants. In previous work, it was demonstrated that *zapC* cells have slightly longer mean lengths (~4.2 μm) than WT cells (~2.9 μm) with a markedly wider range of cell lengths during exponential growth (Durand-Heredia *et al.*, 2012; Hale *et al.*, 2011) (Table 2). Cells with mutations in *clpX*, *clpA* or *clpP* display mean cell lengths statistically similar to those of WT cells, while those with double mutations in *zapC clpX* or *zapC clpA* show little variation in cell lengths compared to those with a mutation in *zapC* alone (Table 2). However, when *zapC* and *clpP* mutations are combined, a synergistic phenotype emerges as seen by the large heterogeneity in the cell lengths observed (~4.3 ± 4.0 μm; maximum filament length up to ~46 μm), which can

Table 2. Cell division phenotypes of *zapC*, *clpX, clpA*, *clpP* and *zapC^{DD}* mutants

Strain	Genotype	Length (μm)*				*n*†
		Mean	SD	Min.	Max.	
MG1655	WT	2.9	0.6	1.8	6.1	89
JD505	*zapC*	4.2	1.7	1.2	29.0	1709
JD407	*clpX*	2.5	0.7	1.5	9.7	555
AJ-S08	*clpA*	3.1	0.8	1.8	7.4	1049
JD409	*clpP*	3.1	0.8	1.3	8.2	587
AC18	*zapC clpX*	4.4	1.7	1.5	20.1	1407
MB103	*zapC clpA*	3.3	1.3	1.6	18.8	900
MB99	*zapC clpP*	4.3	4.0	1.2	45.7	791
MB110	*zapC clpP*/pNG162-*zapC*‡	3.2	1.0	1.5	9.6	544
MB181	*zapC^{DD}*	3.7	1.3	1.4	12.4	1205

*Cells were grown in LB at 37 °C and harvested at OD_{600}=0.6–0.8, immobilized on 1 % agarose pads, and measurements determined using ObjectJ as described. Min. and Max., minimum and maximum cell lengths in the population.
†*n*, total number of cells measured. Less than 100 cells were measured for WT as cell length numbers approximated those described previously under the same conditions.
‡Leaky expression of IPTG-inducible plasmid in pNG162-*zapC* was used.

be rescued by low level expression of ZapC *in trans* (Table 2). Together, the genetic data parallel the antibiotic chase results that ClpX and ClpA may be redundant unfoldases that associate with ClpP and modulate ZapC protein stability.

Chromosomal levels of ZapC^{DD} are stable

Although multicopy ZapC^{DD} was resistant to protease activity, we wanted to address the possibility that ZapC was being targeted for ClpP-mediated degradation due to overproduction from a plasmid-borne system. We therefore examined expression of native levels of ZapC^{DD} upon integration onto the chromosome. ZapC^{DD} levels are stable over 120 min when expressed from the native locus (Fig. 3a). While the chromosomally expressed ZapC^{DD} levels were ~40–50-fold less than that of plasmid-borne ZapC^{DD} expression, we suspect that the enhanced stability of ZapC^{DD} facilitated detection of this protein when expressed in single copy from the chromosome (Figs 3a and S2a). Despite ZapC turnover rates being relatively slow per generation, we failed to reliably detect chromosomally expressed WT ZapC (Fig. 3a). These results support that endogenous ZapC is subject to ClpP-mediated degradation *in vivo*. Despite the high stability of chromosomally encoded ZapC^{DD}, only mild division defects were observed with ~7 % of the cell population being longer compared to mean WT cell lengths (Table 2). The lack of a division phenotype was not simply due to the inability of ZapC^{DD} to interact with FtsZ. We confirmed that similar to WT ZapC, overexpression of ZapC^{DD} results in cell filamentation, a *zapC^{DD}–gfp* fusion localizes to midcell, and ZapC^{DD} interacts with FtsZ and enhances sedimentable FtsZ polymeric mass in an FtsZ-sedimentation assay (Fig. S3). These data indicate that the *zapC^{DD}* mutation does not abrogate interaction of ZapC with FtsZ and that the ClpX and FtsZ interaction domains of ZapC are distinct from each other.

A *zapC^{DD}* mutant promotes Z-ring assembly *in vivo*

As noted previously, increased expression of ClpXP causes a significant proportion of cells to filament, presumably in part due to changes in FtsZ monomer/polymer pools (Table 3) (Camberg *et al.*, 2009). This idea was further supported by the exacerbated division defects displayed by cells lacking ZapC in response to increased levels of ClpXP expression (Table 3). However, ClpXP overexpression in the *zapC^{DD}* background restored WT cell lengths, consistent with ClpXP-mediated degradation of ZapC being a major contributor to the filamentous phenotype resulting from ClpXP overexpression (Table 3).

We next investigated whether a *zapC^{DD}* mutant decreased the thermosensitivity of *ftsZ84* (Ts) cells, as deletion of either *clpX* or *clpP* has been reported to reduce the heat sensitivity of *ftsZ84* (Ts) cells by decreasing the proteolysis of FtsZ84 (Camberg *et al.*, 2011). The well-studied conditional mutant *ftsZ84* (Ts) displays reduced GTPase activity compared to WT FtsZ but divides more or less normally at the permissive temperature (30 °C), although cells are on an average slightly elongated compared to WT cells (Arjes *et al.*, 2015; Powell & Court, 1998). However, *ftsZ84* (Ts) viability decreases at higher temperatures, and FtsZ84 fails to localize to the division site at 42 °C leading to lethal filamentation (RayChaudhuri & Park, 1994; Yu & Margolin, 2000). We used both LB and LBNS media for these assays since LBNS provides a more stringent condition for controlling the expression levels of *ftsZ84* (Ts) as increased intracellular amounts of FtsZ84 can suppress *ftsZ84* (Ts)

Table 3. Cell division phenotypes upon overexpression of ClpXP in WT, *zapC* and $zapC^{DD}$ mutants

Strain	Genotype*	Length (μm)†				*n*‡
		Mean	SD	Min.	Max.	
JD455	WT/pBR322	3.2	0.8	1.4	6.1	525
JD456	WT/pClpXP	6.6	5.3	2.4	59.9	664
AC01-22	*zapC*/pBR322	4.0	1.4	1.9	18.0	730
AC01-20	*zapC*/pClpXP	6.2	7.5	1.5	89.6	687
MB203	$zapC^{DD}$/pClpXP	3.3	0.8	1.7	6.0	449

*Constitutive expression of pClpXP from native promoter in a pBR322 vector backbone in LB at 37 °C
†Cells were harvested at OD_{600}=0.6, immobilized on 1 % agarose pads, and measurements determined using ObjectJ as described. Min. and Max., minimum and maximum cell lengths in the population.
‡*n*, total number of cells measured.

thermosensitivity (Phoenix & Drapeau, 1988; Powell & Court, 1998). We find that stable expression of ZapC, encoded by the chromosomal $zapC^{DD}$ variant, enhances the viability of *ftsZ84* (Ts) cells at 37 °C (Fig. 3b). As shown before, removal of *clpX* or *clpP* also decreased the thermosensitivity of *ftsZ84* (Ts) cells (Fig. 3b) (Camberg *et al.*, 2011). Furthermore, native levels of $zapC^{DD}$ suppress the formation of elongated rods and short filaments in the *ftsZ84* (Ts) background under permissive conditions by ~20 %, and under more stringent conditions, by ~60 % (Fig. 3c). The suppression of *ftsZ84* (Ts) thermosensitive phenotypes is due to increased stability of ZapC, and not because of changes in the intracellular FtsZ amounts, since FtsZ levels in a $zapC^{DD}$ strain are similar to those in WT cells (Fig. S2b). Together, the genetic data support a role for ZapC in stabilizing FtsZ assemblies, and for ClpP-mediated degradation of ZapC to be an important player in modulating FtsZ assembly dynamics.

ZapC turnover rates are not affected by growth rates or growth phase

Although the intracellular concentration of FtsZ remains essentially unchanged at varying growth rates, the frequency of Z-ring formation is altered in a growth-rate-dependent manner, suggesting that FtsZ polymerization dynamics control growth rate regulation of FtsZ-ring formation in *E. coli* (Weart & Levin, 2003). Given that both ClpXP and ZapC regulate Z-ring assembly dynamics, we reasoned that changes in growth rate might differentially influence ClpXP-mediated ZapC stability. To test this hypothesis, we examined ZapC turnover after growth in three different conditions: LB at 37 °C, and M9 minimal glucose (Miller, 1972) at 37 °C and 25 °C. Doubling times in the three conditions were approximately 21, 74 and 255 min, respectively. Our results show that the ClpXP-mediated ZapC degradation rates relative to cell doubling remain unaffected at different cellular generation times, suggesting that changes in ZapC levels do not contribute to the growth-rate regulation of Z-ring formation (Fig. S4).

During stationary phase, protein degradation rates change dependent on the protein substrate, the protease complexes that mediate the degradation, and the nature of the stationary phase (Lies & Maurizi, 2008). Specifically, *ssrA*-tagged substrates are degraded at reduced rates in stationary phase in LB medium due to the reduced activity of ClpXP complexes (Lies & Maurizi, 2008). Although no differential transcriptional activity of *zapC* is seen by Real-TimeqRT-PCR (~0.7-fold change), we examined whether ZapC protein stability was altered in a growth-phase-dependent manner. ZapC turnover rates were similar at OD_{600} ~2.0–3.0 ($t_{1/2}$=121 ± 9 min) to those in exponential growth at OD_{600} ~0.6–0.8 ($t_{1/2}$ =97 ± 21 min), suggesting that ZapC degradation rates remain essentially unaltered in the growth phases tested.

DISCUSSION

ZapC is a positive regulator of FtsZ that binds directly to FtsZ, reduces FtsZ GTPase activity and stabilizes FtsZ lateral assemblies. ClpXP, a conserved protease, controls FtsZ polymer dynamics by degrading FtsZ among other cellular substrates. In this work, we identified a role for the ClpXP protease in ZapC turnover and characterized its consequences on cell division in *E. coli*. Our results show that ZapC is degraded in a ClpP-dependent manner *in vivo*. The adaptor protein SspB is not required for ZapC proteolysis, indicating a direct interaction between the ClpX chaperone and ZapC. Further, the *ssrA*-like C-terminal residues in ZapC serve as a recognition site for ClpXP-mediated degradation. ClpP can also partner with the ATPase ClpA, which overlaps with ClpX in recognition of the *ssrA* tag. Our data indicate that in the absence of ClpX, ClpAP complexes are sufficient for ZapC degradation. Given that in cells lacking both ClpX and ClpA, ZapC levels are stable and similar to levels observed in the absence of ClpP, our results suggest that ZapC is recognized and degraded by both ClpXP and ClpAP complexes *in vivo* likely through recognition of the *ssrA*-like tag (Fig. 4).

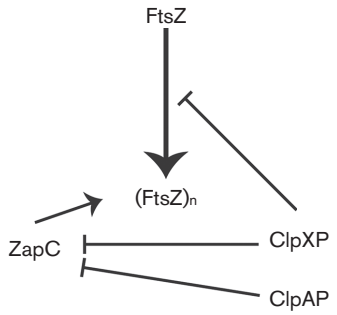

Fig. 4. The molecular interactions between Clp(X/A)P, ZapC and FtsZ in modulating FtsZ-ring assembly in *E. coli*. $(FtsZ)_n$ represents polymeric FtsZ present in the midcell FtsZ-ring. Arrows indicate an interaction leading to enhanced Z-ring polymerization and/or integrity. Blocked lines represent degradation as mediated by ClpXP or ClpAP protease complexes. Although $(FtsZ)_n$ is deemed to be the preferred substrate, ClpXP recognizes either monomeric or polymeric FtsZ, and in this regard influences FtsZ-ring assembly negatively.

The cellular turnover rates of ZapC appear to indicate that ZapC susceptibility to ClpP-mediated degradation is primarily conferred by the *ssrA*-like tag. Recently obtained ZapC crystallographic data are consistent with these results and indicate that ZapC C-terminal residues 167 and after are disordered and could extend far into the solvent making them accessible to ClpX or ClpA (Ortiz *et al.*, 2015; Schumacher *et al.*, 2016). The 11-residue N-terminal peptide (^{1}MRIK-X_6-W^{11}), also predicted to be a ClpX recognition sequence, forms part of a hydrophobic or structural core of the protein and is likely inaccessible (Flynn *et al.*, 2003; Schumacher *et al.*, 2016). Nonetheless, we cannot exclude the possibility that some level of ZapC clearance takes place by recognition of alternative motifs by ClpXP and/or ClpAP protease complexes in the cell. While ClpAP is suggested to degrade only ~5 % of *ssrA*-tagged proteins in WT cells *in vivo*, ZapC encodes for ^{15}EEHDR^{19} residues within the amino terminus, which could potentially serve as a ClpAP recognition target (Hoskins *et al.*, 2000; Lies & Maurizi, 2008). These residues show considerable similarity to the ClpA recognition motif of RepA, a model ClpAP substrate (Hoskins *et al.*, 2000; Lies & Maurizi, 2008). Additionally, degradation of both FtsZ and FtsA by both ClpXP and ClpAP proteases has been demonstrated in *Caulobacter* and *Staphylococcus*, suggesting that multiple protease complexes can contribute to the degradation of FtsZ and other division proteins in the cell (Feng *et al.*, 2013; Williams *et al.*, 2014). Further investigation will be required to dissect the contributions of specific recognition sequences in the ZapC/ClpX or ZapC/ClpA interactions.

Both *E. coli* FtsZ and ZapC are degraded inefficiently by the ClpP protease *in vivo*. In WT cells grown in rich media, FtsZ half-life rates are reported to be ~115 min, and our data show that ZapC clearance rates are between ~80 and 100 min (Camberg *et al.*, 2009). This amounts to 11–17 % degradation of FtsZ and 16–23% degradation of ZapC within one doubling time (20–30 min) in rich medium. Cellular levels of FtsZ are predicted to be ~5000 molecules per cell and changes in FtsZ intracellular concentrations falling below or increasing above the threshold amounts lead to gross division defects or cell death (Wang *et al.*, 1991; Ward & Lutkenhaus, 1985). ZapC is predicted to be a low-abundance protein with ~200 copies per cell and overexpression of ZapC is thought to hyperstabilize aberrant FtsZ assemblies leading to lethal filamentation (Li *et al.*, 2014). Therefore, the relatively slow ClpP-mediated turnover of FtsZ and ZapC per generation suggests that maintaining a fine balance of the FtsZ monomer/polymer ratio and the amounts of the stabilizer ZapC in the cell is critical to Z-ring assembly. Consistent with this model, increased stability of ZapC protects against ClpXP overexpression by stabilizing FtsZ polymer assemblies. This notion was further supported by the ability of native levels of $zapC^{DD}$ to suppress the thermosensitive division phenotypes of *ftsZ84* (Ts) cells. These data also raise the possibility that ClpP-mediated proteolytic control of ZapC can affect cell division differentially under specific conditions where FtsZ monomer/polymer equilibrium is disrupted.

To our knowledge, this is the first report wherein a Z-ring stabilizer, considered to be an accessory divisome component in *E. coli* and related bacteria, is shown to be an intracellular substrate for ClpXP and ClpAP proteases. These results point to at least two levels of regulatory control exercised by proteolysis in Z-ring assembly in *E. coli*: (i) directly on FtsZ and (ii) indirectly through degradation of ZapC. In addition to the heterogeneity of FtsZ regulatory proteins that control Z-ring assembly in different bacteria, data presented here demonstrate additional layers of regulatory inputs, which can provide cells with the necessary flexibility to control Z-ring assembly and optimize survival under rapid environmental fluxes.

ACKNOWLEDGEMENTS

We are grateful to Tom Bernhardt, Michael Maurizi and Scot Ouellette for generous gifts of plasmids, strains and antibody; Daniel Haeusser and Seth Goldman for providing critical comments on the manuscript; and Jorge Durand-Heredia and Helene Vase-Frandsen for technical assistance. This work was supported by a US DOE graduate stipend (GAANN P200A120211 to M. S. B.) and an NSF award (MCB 1158059 to A. J.). An NIMHD grant (8G12MD007603-29) provides core facility support to the City College of New York.

REFERENCES

Adams, D. W. & Errington, J. (2009). Bacterial cell division: assembly, maintenance and disassembly of the Z ring. *Nat Rev Microbiol* **7**, 642–653.

Arjes, H. A., Lai, B., Emelue, E., Steinbach, A. & Levin, P. A. (2015). Mutations in the bacterial cell division protein FtsZ highlight the role of GTP binding and longitudinal subunit interactions in assembly and function. *BMC Microbiol* **15,** 209.

Baker, T. A. & Sauer, R. T. (2012). ClpXP, an ATP-powered unfolding and protein-degradation machine. *Biochim Biophys Acta* **1823**, 15–28.

Bernhardt, T. G. & de Boer, P. A. J. (2004). Screening for synthetic lethal mutants in *Escherichia coli* and identification of EnvC (YibP) as a periplasmic septal ring factor with murein hydrolase activity. *Mol Microbiol* **52**, 1255–1269.

Bi, E. F. & Lutkenhaus, J. (1991). FtsZ ring structure associated with division in *Escherichia coli*. *Nature* **354**, 161–164.

Camberg, J. L., Hoskins, J. R. & Wickner, S. (2009). ClpXP protease degrades the cytoskeletal protein, FtsZ, and modulates FtsZ polymer dynamics. *Proc Natl Acad Sci U S A* **106**, 10614–10619.

Camberg, J. L., Hoskins, J. R. & Wickner, S. (2011). The interplay of ClpXP with the cell division machinery in *Escherichia coli*. *J Bacteriol* **193**, 1911–1918.

Camberg, J. L., Viola, M. G., Rea, L., Hoskins, J. R. & Wickner, S. (2014). Location of dual sites in *E. coli* FtsZ important for degradation by ClpXP; one at the C-terminus and one in the disordered linker. *PLoS One* **9**, e94964.

Dajkovic, A., Mukherjee, A. & Lutkenhaus, J. (2008). Investigation of regulation of FtsZ assembly by SulA and development of a model for FtsZ polymerization. *J Bacteriol* **190**, 2513–2526.

Datsenko, K. A. & Wanner, B. L. (2000). One-step inactivation of chromosomal genes in *Escherichia coli* K-12 using PCR products. *Proc Natl Acad Sci U S A* **97**, 6640–6645.

de Boer, P. A. J. (2010). Advances in understanding *E. coli* cell fission. *Curr Opin Microbiol* **13**, 730–737.

Durand-Heredia, J. M., Yu, H. H., De Carlo, S., Lesser, C. F. & Janakiraman, A. (2011). Identification and characterization of ZapC, a stabilizer of the FtsZ ring in *Escherichia coli*. *J Bacteriol* **193**, 1405–1413.

Durand-Heredia, J., Rivkin, E., Fan, G., Morales, J. & Janakiraman, A. (2012). Identification of ZapD as a cell division factor that promotes the assembly of FtsZ in *Escherichia coli*. *J Bacteriol* **194**, 3189–3198.

Dziedzic, R., Kiran, M., Plocinski, P., Ziolkiewicz, M., Brzostek, A., Moomey, M., Vadrevu, I. S., Dziadek, J., Madiraju, M. & other authors (2010). *Mycobacterium tuberculosis* ClpX interacts with FtsZ and interferes with FtsZ assembly. *PLoS One* **5**, e11058.

Erickson, H. P., Anderson, D. E. & Osawa, M. (2010). FtsZ in bacterial cytokinesis: cytoskeleton and force generator all in one. *Microbiol Mol Biol Rev* **74**, 504–528.

Feng, J., Michalik, S., Varming, A. N., Andersen, J. H., Albrecht, D., Jelsbak, L., Krieger, S., Ohlsen, K., Hecker, M. & other authors (2013). Trapping and proteomic identification of cellular substrates of the ClpP protease in *Staphylococcus aureus*. *J Proteome Res* **12**, 547–558.

Flynn, J. M., Neher, S. B., Kim, Y. I., Sauer, R. T. & Baker, T. A. (2003). Proteomic discovery of cellular substrates of the ClpXP protease reveals five classes of ClpX-Recognition signals.. *Mol Cell* **11**, 671–683.

Goehring, N. W., Gonzalez, M. D. & Beckwith, J. (2006). Premature targeting of cell division proteins to midcell reveals hierarchies of protein interactions involved in divisome assembly. *Mol Microbiol* **61**, 33–45.

Gottesman, S., Wickner, S., Jubete, Y., Singh, S. K., Kessel, M. & Maurizi, M. (1995). Selective, energy-dependent proteolysis in *Escherichia coli*. *Cold Spring Harb Symp Quant Biol* **60**, 533–548.

Haeusser, D. P., Lee, A. H., Weart, R. B. & Levin, P. A. (2009). ClpX inhibits FtsZ assembly in a manner that does not require its ATP hydrolysis-dependent chaperone activity. *J Bacteriol* **191**, 1986–1991.

Hale, C. A., Shiomi, D., Liu, B., Bernhardt, T. G., Margolin, W., Niki, H. & de Boer, P. A. J. (2011). Identification of *Escherichia coli* ZapC (YcbW) as a component of the division apparatus that binds and bundles FtsZ polymers. *J Bacteriol* **193**, 1393–1404.

Haney, S. A., Glasfeld, E., Hale, C. A., Keeney, D., He, Z. & de Boer, P. A. J. (2001). Genetic analysis of the *Escherichia coli* FtsZ.ZipA interaction in the yeast two-hybrid system. Characterization of FtsZ residues essential for the interactions with ZipA and with FtsA. *J Biol Chem* **276**, 11980–11987.

Hoskins, J. R., Kim, S. Y. & Wickner, S. (2000). Substrate recognition by the ClpA chaperone component of ClpAP protease. *J Biol Chem* **275**, 35361–35367.

Huang, K. H., Durand-Heredia, J. & Janakiraman, A. (2013). FtsZ ring stability: of bundles, tubules, crosslinks, and curves. *J Bacteriol* **195**, 1859–1868.

Karimova, G., Pidoux, J., Ullmann, A. & Ladant, D. (1998). A bacterial two-hybrid system based on a reconstituted signal transduction pathway. *Proc Natl Acad Sci U S A* **95**, 5752–5756.

Karimova, G., Ullmann, A. & Ladant, D. (2000). A bacterial two-hybrid system that exploits a cAMP signaling cascade in *Escherichia coli*. *Methods Enzymol* **328**, 59–73.

Karzai, A. W., Roche, E. D. & Sauer, R. T. (2000). The SsrA-SmpB system for protein tagging, directed degradation and ribosome rescue. *Nat Struct Biol* **7**, 449–455.

Keiler, K. C., Waller, P. R. & Sauer, R. T. (1996). Role of a peptide tagging system in degradation of proteins synthesized from damaged messenger RNA. *Science* **271**, 990–993.

Levchenko, I., Seidel, M., Sauer, R. T. & Baker, T. A. (2000). A specificity-enhancing factor for the ClpXP degradation machine. *Science* **289**, 2354–2356.

Li, G. W., Burkhardt, D., Gross, C. & Weissman, J. S. (2014). Quantifying absolute protein synthesis rates reveals principles underlying allocation of cellular resources. *Cell* **157**, 624–635.

Lies, M. & Maurizi, M. R. (2008). Turnover of endogenous SsrA-tagged proteins mediated by ATP-dependent proteases in *Escherichia coli*. *J Biol Chem* **283**, 22918–22929.

Lutkenhaus, J. F. & Donachie, W. D. (1979). Identification of the *ftsA* gene product. *J Bacteriol* **137**, 1088–1094.

Lutkenhaus, J., Pichoff, S. & Du, S. (2012). Bacterial cytokinesis: Z ring to divisome. *Cytoskeleton (Hoboken)* **69**, 78–90.

Miller, J. (1972). *Experiments in Molecular Genetics*. New York: Cold Spring Harbor Laboratory.

Mukherjee, A. & Lutkenhaus, J. (1998). Dynamic assembly of FtsZ regulated by GTP hydrolysis. *EMBO J* **17**, 462–469.

Neher, S. B., Villén, J., Oakes, E. C., Bakalarski, C. E., Sauer, R. T., Gygi, S. P. & Baker, T. A. (2006). Proteomic profiling of ClpXP substrates after DNA damage reveals extensive instability within SOS regulon. *Mol Cell* **22**, 193–204.

Ortiz, C., Kureisaite-Ciziene, D., Schmitz, F., McLaughlin, S. H., Vicente, M. & Löwe, J. (2015). Crystal structure of the Z-ring associated cell division protein ZapC from *Escherichia coli*. *FEBS Lett* **589**, 3822–3828.

Ortiz, C., Natale, P., Cueto, L. & Vicente, M. (2016). The keepers of the ring: regulators of FtsZ assembly. *FEMS Microbiol Rev* **40**, 57–67.

Park, K. T., Wu, W., Battaile, K. P., Lovell, S., Holyoak, T. & Lutkenhaus, J. (2011). The Min oscillator uses MinD-dependent conformational changes in MinE to spatially regulate cytokinesis. *Cell* **146**, 396–407.

Pazos, M., Natale, P. & Vicente, M. (2013). A specific role for the ZipA protein in cell division: stabilization of the FtsZ protein. *J Biol Chem* **288**, 3219–3226.

Peters, N. T., Dinh, T. & Bernhardt, T. G. (2011). A fail-safe mechanism in the septal ring assembly pathway generated by the sequential recruitment of cell separation amidases and their activators. *J Bacteriol* **193**, 4973–4983.

Phoenix, P. & Drapeau, G. R. (1988). Cell division control in *Escherichia coli* K-12: some properties of the *ftsZ84* mutation and suppression of this mutation by the product of a newly identified gene. *J Bacteriol* **170**, 4338–4342.

Pichoff, S. & Lutkenhaus, J. (2005). Tethering the Z ring to the membrane through a conserved membrane targeting sequence in FtsA. *Mol Microbiol* **55**, 1722–1734.

Powell, B. S. & Court, D. L. (1998). Control of *ftsZ expression,* cell division, and glutamine metabolism in Luria-Bertani medium by the alarmone ppGpp in *Escherichia coli*. *J Bacteriol* **180**, 1053–1062.

Raskin, D. M. & de Boer, P. A. J. (1999). MinDE-dependent pole-to-pole oscillation of division inhibitor MinC in *Escherichia coli*. *J Bacteriol* **181**, 6419–6424.

RayChaudhuri, D. & Park, J. T. (1994). A point mutation converts *Escherichia coli* FtsZ septation GTPase to an ATPase. *J Biol Chem* **269**, 22941–22944.

Rueda, S., Vicente, M. & Mingorance, J. (2003). Concentration and assembly of the division ring proteins FtsZ, FtsA, and ZipA during the *Escherichia coli* cell cycle. *J Bacteriol* **185**, 3344–3351.

Schumacher, M. A., Zeng, W., Huang, K. H., Tchorzewski, L. & Janakiraman, A. (2016). Structural and functional analyses reveal insights into the molecular properties of the *Escherichia coli* Z ring stabilizing protein ZapC. *J Biol Chem* **291**, 2485–2498.

Shen, B. & Lutkenhaus, J. (2009). The conserved C-terminal tail of FtsZ is required for the septal localization and division inhibitory activity of MinC(C)/MinD. *Mol Microbiol* **72**, 410–424.

Wang, X. D., de Boer, P. A. J. & Rothfield, L. I. (1991). A factor that positively regulates cell division by activating transcription of the major cluster of essential cell division genes of *Escherichia coli*. *EMBO J* **10**, 3363–3372.

Ward, J. E. & Lutkenhaus, J. (1985). Overproduction of FtsZ induces minicell formation in *E. coli*. *Cell* **42**, 941–949.

Weart, R. B. & Levin, P. A. (2003). Growth rate-dependent regulation of medial FtsZ ring formation. *J Bacteriol* **185**, 2826–2834.

Weart, R. B., Nakano, S., Lane, B. E., Zuber, P. & Levin, P. A. (2005). The ClpX chaperone modulates assembly of the tubulin-like protein FtsZ. *Mol Microbiol* **57**, 238–249.

Wickner, S., Maurizi, M. R. & Gottesman, S. (1999). Posttranslational quality control: folding, refolding, and degrading proteins. *Science* **286**, 1888–1893.

Williams, B., Bhat, N., Chien, P. & Shapiro, L. (2014). ClpXP and ClpAP proteolytic activity on divisome substrates is differentially regulated following the *Caulobacter* asymmetric cell division. *Mol Microbiol* **93**, 853–866.

Yu, X. C. & Margolin, W. (2000). Deletion of the *min* operon results in increased thermosensitivity of an *ftsZ84* mutant and abnormal FtsZ ring assembly, placement, and disassembly. *J Bacteriol* **182**, 6203–6213.

Edited by: S. Frank